12. J. Li, S. H. Yang, C. M. Zhao, H. Y. Zhang, and W. Xie, "High efficient single-frequency output at 1991 nm from a diode-pumped Tm:YAP coupled cavity," Opt. Express **18**(12), 12161–12167 (2010).
13. P. Cemy and D. Burns, "Modeling and experimental investigation of a diode-pumped Tm:YAlO₃ laser with a- and b-cut crystal orientations," IEEE J. Sel. Top. Quantum Electron. **11**(3), 674–681 (2005).
14. I. F. Elder and M. J. P. Payne, "Lasing in diode-pumped Tm:YAP, Tm,Ho:YAP and Tm,Ho:YLF," Opt. Commun. **145**(1-6), 329–339 (1998).
15. B. Q. Yao, L. J. Li, L. L. Zheng, Y. Z. Wang, G. J. Zhao, and J. Xu, "Diode-pumped continuous wave and Q-switched operation of a c-cut Tm,Ho:YAlO(₃) laser," Opt. Express **16**(7), 5075–5081 (2008).
16. L. J. Li, B. Q. Yao, C. W. Song, Y. Z. Wang, and Z. G. Wang, "Continuous wave and AO Q-switch operation Tm,Ho:YAP laser pumped by a laser diode of 798nm," Laser Phys. Lett. **6**(2), 102–104 (2009).
17. L. J. Li, B. Q. Yao, Y. L. Ju, Y. J. Zhang, and Y. Z. Wang, "Dual diodes end-pumped Q-switch operation of a c-cut 2044-nm Tm,Ho:YAlO₃ laser," Laser Phys. Lett. **6**(5), 367–369 (2009).
18. L. J. Li, B. Q. Yao, Z. G. Wang, X. M. Duan, G. Li, and Y. Z. Wang, "Continuous wave and AO Q-switch operation of a b-cut Tm,Ho:YAP laser with dual wavelengths pumped by a laser diode of 792nm," Laser Phys. **20**(1), 205–208 (2010).
19. K. Yang, H. Bromberger, H. Ruf, H. Schäfer, J. Neuhaus, T. Dekorsy, C. V.-B. Grimm, M. Helm, K. Biermann, and H. Künzel, "Passively mode-locked Tm,Ho:YAG laser at 2 μm based on saturable absorption of intersubband transitions in quantum well," Opt. Express **18**(7), 6537–6544 (2010).
20. Z. Wang, B. Yao, G. Li, Y. Ju, and Y. Wang, "Single longitudinal mode lasing of Tm,Ho:YAP microchip laser at 2000.4 nm," Laser Phys. **20**(2), 458–461 (2010).
21. G. Li, B. Yao, Z. Jiang, X. Duan, Z. Wang, Y. Ju, and Y. Wang, "Compact diode end-pumped c-cut Tm,Ho:YAlO₃ laser," Laser Phys. **19**(12), 2151–2154 (2009).
22. S. Verghese, K. A. McIntosh, and E. R. Brown, "Optical and terahertz power limits in the low-temperature-grown GaAs photomixers," Appl. Phys. Lett. **71**(19), 2743 (1997).

1. Introduction

Laser sources operating in the 2 μm eye-safe region are promising candidates for various applications in LIDAR, laser ranging, high-resolution spectroscopy, frequency metrology, laser microsurgery and optical communication. They are also of interest for pumping of optical parametric oscillators (OPOs) and solid state lasers farther in mid-infrared range, which have a growing number of applications in spectroscopy, medicine and defense [1,2]. Tm,Ho co-doped solid state lasers generating 2 μm radiation, such as Tm,Ho co-doped YAG [3], YLiF$_4$ [4,5], LuLiF$_4$ [5] and GdVO$_4$ [6], etc., attract a lot of interest due to the remarkable properties including a quantum efficiency of nearly two via cross relaxation and an enhanced energy storage associated with a long upper-level lifetime.

The laser host yttrium aluminum oxide (YAlO$_3$), short YALO or YAP, is a biaxial crystal with the orthorhombic D$^{16}_{2h}$ space group and the lattice constants of a = 5.329 Å, b = 7.730 Å, c = 5.179 Å [7]. YAP is derived from the same binary Y$_2$O$_3$–Al$_2$O$_3$ systems as the common host YAG, so it has similar physical properties, such as high mechanical strength, sufficient hardness and significant thermal characteristics [8]. However, compared with YAG host, YAP has natural birefringence that dominates any thermally induced birefringence due to the anisotropic structure, even when the YAP crystal is doped with rare earth ions and pumped at high power [9]. As a result, thermally induced degradation is prevented intrinsically and linearly polarized emission is easily available from YAP lasers. Therefore, YAP crystals become a potentially useful laser host for thulium and holmium doping. It is important to note that the $^3H_6 \rightarrow ^3H_4$ absorption transition of thulium doped in a YAP host possesses a strong absorption peak with a FWHM of about 4 nm in all crystalline orientations at around 795 nm. This is significantly broader than that in YAG at 785 nm [10] and greatly decreases the strictness of the requirements of GaAs/AlGaAs laser diodes for pumping. So far, diode-pumped thulium doped YAP lasers [11–13] and thulium sensitized holmium doped YAP lasers [14–18], both in continuous wave and Q-switch operation regimes, have been demonstrated by several groups. The anisotropic structure makes the absorption and gain properties of YAP host based lasers polarization dependent, the laser performance is therefore influenced by the crystal orientation. Cerny *et al.* have demonstrated a comparative study of Tm:YAP lasers in *a*- and *b*-cut orientation, and the results showed that *a*-cut oriented Tm:YAP crystal could give superior performance at the emission wavelength of 1.98 μm than that of the *b*-cut orientation at 1.94 μm [13]. Despite the number of publications on

Tm,Ho:YAP lasers [14–18], the reports almost all focused on the *b*-cut and *c*-cut oriented crystals. By using *b*-cut oriented crystals, emission wavelengths of 2000 nm, 2129 nm and 2120 nm have been obtained with optical-to-optical conversion efficiency from 1.6% to 26.5% under continuous wave operation regime. With *c*-cut crystals, emission wavelengths of 2130 nm, 2132 nm and 2044 nm have been achieved with optical-to-optical conversion efficiency from 15.4% to 31.3%. Furthermore, most of the Tm,Ho:YAP lasers worked with liquid nitrogen cooling. However, to our best knowledge, experimental investigation on an *a*-cut Tm,Ho:YAP laser at room temperature are not yet available.

In this paper we have investigated the laser performance of Tm,Ho:YAP lasers end-pumped by a wavelength tunable Ti-sapphire laser, in which the crystals with optical axis oriented parallel to the crystallographic *a* and *b* axes were employed. The impact of the crystal orientations on the laser output characteristics such as lasing threshold, output power, optical-to-optical conversion efficiency and output wavelength have been studied experimentally.

2. Experiments and discussions

The laser crystals used in this paper were grown by the Czochralski technique. One is grown along the crystalline *a*-axis for YAP host, and the other one *b*-cut oriented. Both the *a*-cut and *b*-cut oriented crystals were with 5at.% thulium and 0.3at.% holmium doped, however, with different size of $4 \times 4 \times 10$ mm^3 and $4 \times 4 \times 8$ mm^3, respectively. Both crystals had antireflection coating on both flat-polished parallel facets from 750 to 850 nm (reflectivity < 2%) and 1930-2230 nm (reflectivity < 0.8%). The laser crystals were wrapped in Indium foil to increase thermal contact and mounted in a copper holder and water-cooled to 12°C. The schematic laser setup employed in the experiment is shown in Fig. 1. In order to overcome the lower laser level population and achieve lasing thresholds at room temperature, a wavelength tunable continuous wave Ti:Sapphire laser was employed as the pump source with a maximum output power of 3 W at 785 nm. The output beam from the Ti:Sapphire laser had a horizontal polarization direction and the output wavelength ranged from 726 nm to 859 nm. The M^2 factor of the pump beam was measured to be about 1.2 and 1.3 in the sagittal and tangential planes, respectively. The pump beam was focused into the gain medium by using a lens with a focal length of 50 mm. The Tm,Ho:YAP crystals were placed at the center of the cavity arm formed by mirror M$_1$ and M$_2$, which had the same radii of curvature of 100 mm and a reflectivity of 99.9% from 2010 to 2100 nm. In addition, the front surface of mirror M$_1$ was high transmission coated at the central wavelength of 785 nm to improve the pump coupling efficiency. Mirrors M$_3$ and M$_4$, with the same radii of curvature of 50 mm, formed another cavity arm providing flexibility of varying laser mode radii in Tm,Ho:YAP crystals to realize good matching between the oscillating mode and pump beam.
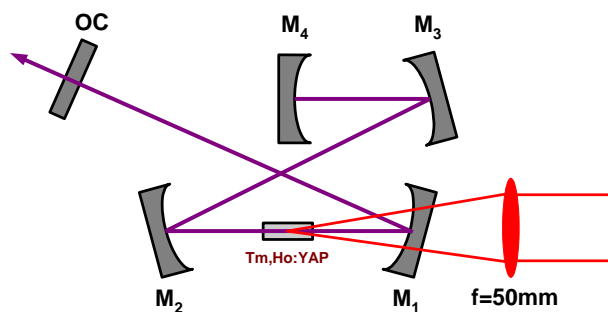

Fig. 1. Schematic setup of continuous wave operation Tm,Ho:YAP laser. OC: output coupler.

2.1 Absorption properties of a- *and* b-*cut Tm,Ho:YAP crystals*

To evaluate the absorption properties of Tm,Ho:YAP crystals with different orientations, the polarized absorption spectrum of the *a*- and *b*-cut Tm,Ho:YAP crystals were measured first at room temperature by using a Fourier-Transform Spectrometer (Vertex FTIR, Bruker Inc.). In order to perform polarization dependent measurements, a polarizer was used to select horizontal and vertical polarization components of the white light source. The beam diameter used to measure the wavelength dependent transmission of the laser crystals was about 2.5 mm. The measured room temperature absorption for the two crystals and both polarizations is shown in Fig. 2. With polarized pump light of E//*c*, the absorption peak value of 5.25 cm^{-1} at 795 nm was a little smaller than that of 5.35 cm^{-1} with E//*b* for *a*-cut Tm,Ho:YAP crystal. In addition, it was found that the E//*c* absorption line at 795 nm was narrower than that of E//*b*. As for *b*-cut crystal, there were two absorption peak values of 6.16 cm^{-1} and 6.32 cm^{-1} locating at 793.7 nm and 799.4 nm, respectively, when polarized pump light of E//*a* was used, both of which were a little lower than that of 6.4 cm^{-1} at 795 nm in the case of E//*c*. In our experiment, the *c*-axis of both crystals was parallel to the horizontal polarization direction of the pump light from the Ti-Sapphire laser to compare the lasing performance of *a*- and *b*-cut crystals conveniently.
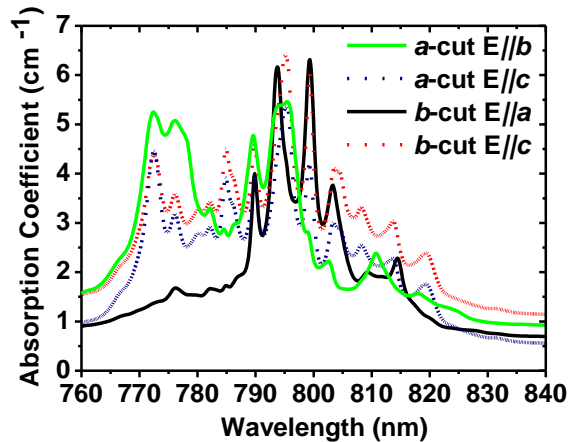

Fig. 2. Polarized absorption spectrum of Tm(5 at. %),Ho(0.3 at. %):YAP crystals at room temperature.

Although the absorption properties without lasing were investigated, we still experimentally measured the absorption coefficients and optical-to-optical conversion efficiencies of both crystals in the lasing situations. In each measurement, the absorbed pump power was calculated by the difference between the incident pump power on the crystal and the leaking power after the mirror M$_2$. The pump light absorption coefficients of the crystals were measured at different pump wavelengths of the cw Ti:Sapphire laser built by ourselves. Due to the inaccuracy of the tunability, the employed pump wavelength was not varied accurately. Among the pump wavelengths available in our experiments, a maximum absorption with coefficient of 2.78 cm^{-1} for the *a*-cut orientation crystal occurs at 793 nm, whereas the *b*-cut one shows a maximum absorption coefficient of 4.45 cm^{-1} at 794.6 nm. Under the same pump wavelength, the absorption coefficients of both crystals under lasing situation were lower than those under non-lasing as shown in the upper inset of Fig. 3. By measuring the output powers and comparing with the absorbed pump power under different pump wavelengths, the dependence of optical-to-optical conversion efficiencies on the pump wavelengths was obtained as shown in the lower inset of Fig. 3. The optical conversion

efficiency curves of both crystals show a flat top, despite the *a*-cut crystal demonstrating slightly higher efficiency than the *b*-cut one. By simultaneously considering the pump light absorption coefficients and the optical-to-optical conversion efficiencies of the laser crystals, we employed the pump wavelength of 783.1 nm for *a*-cut crystal, and 794.6 nm for *b*-cut crystal for the following experiments, respectively.
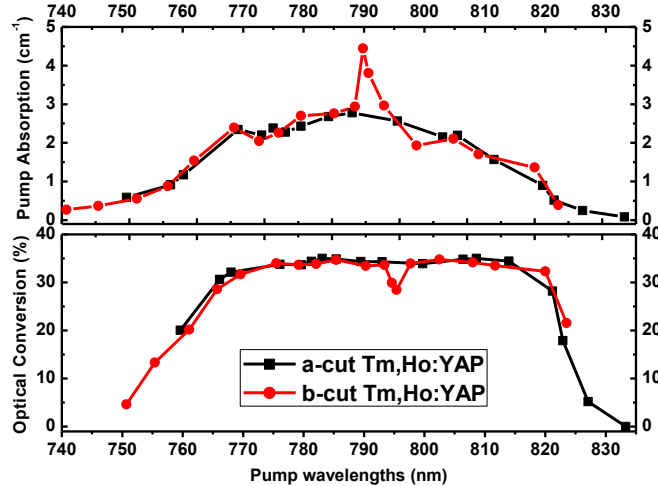

Fig. 3. Dependences of absorption coefficients and optical conversion efficiencies on different pump wavelengths for *a*- and *b*-cut Tm,Ho:YAP crystals under lasing situation with polarized pump light of E//*c*. upper inset: absorption coefficients; lower inset: optical conversion efficiencies.

2.2 Laser performance of a- and b-cut crystals

Due to the serious reabsorption loss in Ho ions, Yao et al. found that the diode-pumped *c*-cut Tm,Ho:YAP laser could not run at room temperature [15]. However, both *a*- and *b*-cut Tm,Ho:YAP lasers could easily run at room temperature of 12°C in our experiment probably because of the high-brightness pump beam from the Ti:Sapphire laser source. Each crystal was measured in turn by using four output couplers (OCs) with different transmissions of 0.5%, 2%, 3% and 5% at 2 μm to find the most efficient configuration. With carefully aligning the cavity to achieve maximum output power for the *a*- and *b*-cut Tm,Ho:YAP crystal, we measured the output spectra by using a laser spectrometer with a resolution bandwidth of 0.4 nm (APE WaveScan, APE Inc.). In free running continuous wave operation, the output spectra show that both the *a*- and *b*-cut Tm,Ho:YAP lasers could emit single emission wavelengths at around 2103 nm and 2129 nm, which did not vary with different output couplers and pump powers. Under single wavelength operation, we recorded the continuous wave output powers for each crystal. Due to different absorption properties of the crystals and pump wavelengths, the absorbed power varied from one sample to the other. To compare the laser performance of the samples, the resulting output powers are plotted as a function of the absorbed power with different output couplers and are shown in Fig. 4. For these measurements the laser cavity was optimized first for the different output couplers at maximum pump power and then the pump power was reduced successively to the threshold pump power. While reducing the power no more changes to the cavity were applied.

In the case of the *a*-cut Tm,Ho:YAP crystal, the fitted threshold pump powers were 472 mW, 681 mW, 466 mW, and 779 mW at the pump wavelength of 783.1 nm for the respective output couplers of T = 0.5%, 2%, 3%, and 5%. A maximum slope efficiency of 45.9% for *a*-cut Tm,Ho:YAP crystal was obtained with output coupler of T = 5%, corresponding to a

maximum output power of 890mW and an optical-to-optical conversion efficiency of 32.2%. Whereas for the *b*-cut crystal, the fitted threshold pump powers were 645 mW, 517 mW, 558 mW, 677 mW at a pump wavelength of 794.6 nm for the respective output couplers of T = 0.5%, 2%, 3%, and 5%. A maximum slope efficiency of 40.9% for the *b*-cut Tm,Ho:YAP crystal was obtained with output coupler of T = 3%, corresponding to a maximum output power of 946 mW and an optical conversion efficiency of 33.1%. The dependence of optical conversion efficiencies on the absorbed pump powers is also shown in Fig. 4. These demonstrated efficiencies for both *a*- and *b*-cut Tm,Ho:YAP crystals are superior to the room temperature operation reported by Li *et al.* with a slope efficiency of 32.4% and an optical-to-optical conversion efficiency of 29.6% [16].
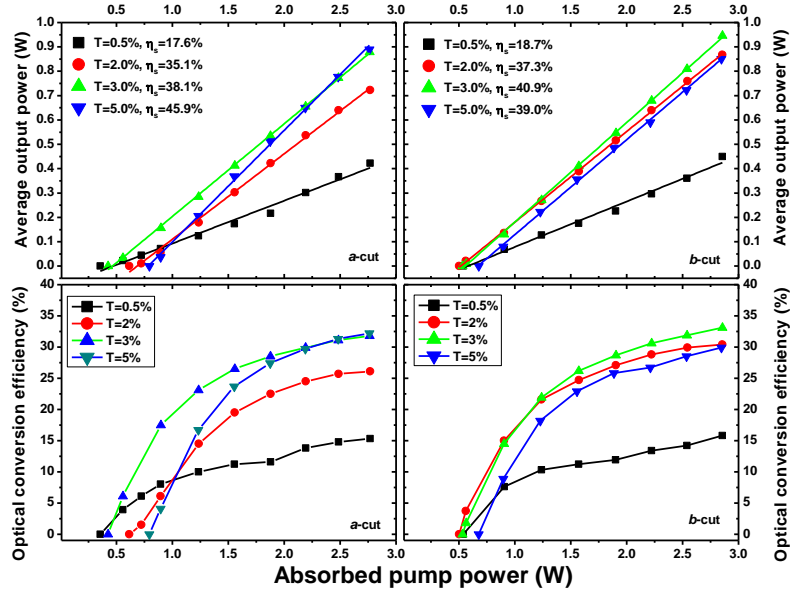

Fig. 4. The average output powers and optical conversion efficiencies versus the absorbed pump power under different output couplers in free running continuous wave operation.

Utilizing the fitted slope efficiency, η_s, for output couplers given in Fig. 4, the intrinsic intracavity loss, *L*, and pump quantum efficiency, η_q, can be calculated from [10,15]

$$\eta_s = \eta_p \frac{v_L}{v_P} \frac{T}{T+L},$$

where v_L is the frequency of the emitted laser light, v_P is the frequency of the pump light and *T* is the transmission of the output coupler. For the *a*-cut Tm,Ho:YAP crystal with a pump wavelength of 783.1 nm and a lasing wavelength of 2119 nm, this results in a quantum efficiency of $\eta_q = 1.48$ and an intrinsic loss of $L = 1.1\%$, whereas a quantum efficiency of $\eta_q = 1.43$ and an intrinsic loss of $L = 0.9\%$ is obtained for the *b*-cut crystal with a pump wavelength of 794.6 nm and lasing wavelength of 2103 nm. The calculated quantum efficiencies for both *a*- and *b*-cut Tm,Ho:YAP crystals are higher than the calculated value of 1.32 for a YAG crystal in our previous work under a similar laser configuration [19]. Stoneman *et al.* [10] and Cerny *et al.* [13] have experimentally and theoretically demonstrated that the emission wavelength of a Tm:YAP laser depends on the crystal orientation, crystal length and the amount of intrinsic cavity loss. The output wavelengths have been investigated for *a*- and *b*-cut Tm,Ho:YAP crystals while varying the intracavity loss induced by inserting an additional thin plate of fused silica into the cavity at Brewster angle. After inserting the fused silica

plate, the *a*-cut Tm,Ho:YAP laser was found to emit at wavelengths around 2103 nm and 2130 nm, singly and simultaneously, respectively, by carefully changing the inserted angle under different output couplers. However, we could not obtain the emission wavelength of 2119 nm, which was easily achieved in free running regime. When the *a*-cut Tm,Ho:YAP laser run at 2103 nm singly, the output powers under different output couplers and pump powers were recorded as shown in Fig. 5. The corresponding optical-to-optical conversion efficiencies were calculated and also demonstrated in Fig. 5. At the single output wavelength of 2130 nm, the output powers were measured only with output couplers of T = 0.5% and 2%, whereas the case with output coupler of T = 5% was not recorded due to a very low output power of several mWs, which was probably caused by high loss and low emission cross section at 2130 nm of the crystal. Maximum output powers of 836 mW at 2103 nm and 487 mW at 2130 nm were obtained, corresponding to an optical conversion efficiencies of 31% and 18%, respectively.
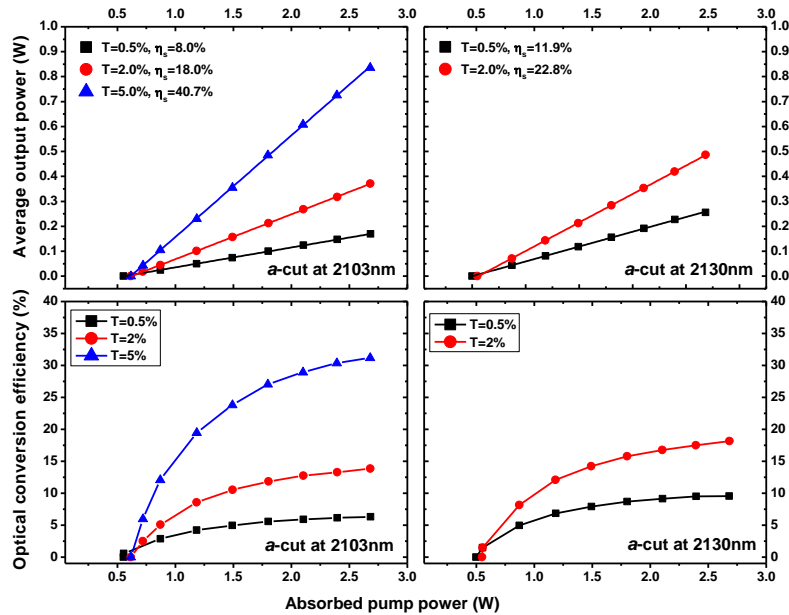

Fig. 5. The output powers of *a*-cut Tm,Ho:YAP laser at different emission wavelengths.

With the *b*-cut crystal employed as the gain medium, a single emission wavelength of 2103 nm could always be obtained under the output couplers of T = 2%, 3% and 5% when the thin plate of fused silica was inserted into the cavity. However, when the coupler of T = 0.5% was employed, single- and dual-wavelength operations at 2103 nm and 2130 nm could be achieved. At the single wavelength operation of 2130 nm, the maximum output power of 221 mW at the absorbed pump power of 2.85 W corresponded to an optical conversion efficiency of 7.7%. In addition, by removing the fused silica plate from the *b*-cut Tm,Ho:YAP laser, we observed single-wavelength operation at 2096 nm and dual-wavelength operation with 2096 and 2103 nm by tuning the output mirror carefully when the output coupler of T = 3% and 5% were employed. However, the corresponding output powers were very low. Furthermore, as we changed the pump wavelength to 783.1 nm, dual-wavelength operations of 2103/2129 nm, 2096/2103 nm, 2103/2061 nm, 2061/2096 nm and 2061/2103 nm as well as a triple-wavelength operation of 2061/2096/2103 nm were observed by carefully tuning the output coupler. However, we did not find the spectra of 2061 nm and 2096 nm when we placed the fused silica plate into the cavity, probably because the induced intracavity loss by the fused silica plate suppressed the oscillations at these wavelengths. The summarized output spectra

of *a*-cut and *b*-cut Tm,Ho:YAP crystals under single- and multi-wavelength operation regimes are shown in Fig. 6. From Fig. 6, we can see that new lasing wavelengths of 2061 nm, 2096 nm and 2103 nm for Tm,Ho:YAP lasers have been achieved, compared with the reported output wavelengths of 2000.4 nm [20], 2040 nm and 2100 nm [21], 2044 nm [17], 2120 nm [14] and 2130 nm [16,21].

The difference in output wavelength can be explained by the round trip loss, that is, the mode with the least loss or the lowest threshold oscillates. Therefore, the laser output wavelength is determined by the particular transition which reaches its threshold first. According to the expression for the threshold pump power shown in [10], to theoretically investigate the detailed dependence of output lasing spectra on the intracavity loss, the emission cross-section of the laser medium should be measured. However, due to the lack of such data for our crystals, we could only experimentally demonstrate the variations of output spectra with the conditions of pump wavelength, intracavity loss etc. However, such work is underway.
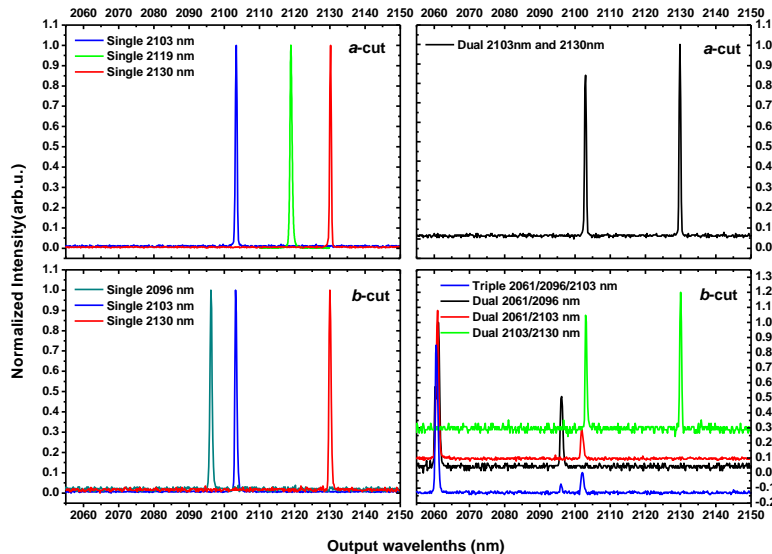

Fig. 6. Output spectra for single and multi-wavelength operation in the *a*- and *b*-cut Tm,Ho:YAP crystals. In the lower right graph the curves are vertically off-set for clarity.

3. Conclusion

To our knowledge, this paper is the first to report on a comparative study of Tm,Ho:YAP lasers in *a*- and *b*-cut orientation. Output powers of 890 mW for *a*-oriented Tm,Ho:YAP crystal at 2119 nm as well as about 950 mW for *b*-oriented Tm,Ho:YAP crystal at 2103 nm were achieved. The maximum slope efficiency in terms of absorbed pump power nearly reached 46% for the *a*-oriented crystal and about 41% for the *b*-oriented crystal. The crystals basically demonstrate similar performance in terms of output power and optical conversion efficiency, although the *a*-cut orientation Tm,Ho:YAP crystal gives a higher maximum slope efficiency over the *b*-cut orientation without considering emission wavelength and crystal length. In addition, the *a*-cut crystal shows a broader absorption peak, which makes it more suitable for being pumped by high power diodes. By inserting a fused silica plate to vary the intracavity loss, a regime of dual-wavelength operations for *a*-oriented crystal were obtained, and for the *b*-oriented crystal, four dual-wavelength operations as well as one configuration of triple-wavelength operation were achieved. Considering this, the *b*-cut orientation crystal demonstrates more plentiful multi-wavelength operations than the *a*-cut orientation, however,

both orientated crystals can provide efficient ways to realize multi-wavelength lasing operation at 2 μm. This might be particularly interesting for generation of terahertz radiation by the means of difference frequency mixing [22], since the conversion efficiency of difference frequency mixing increases with lower frequency and the photon energy is less than twice the band gap of common semiconductors used for the generation, thus higher pump powers can be used.

Acknowledgments